https://doi.org/10.5194/egusphere-2026-834
Preprint. Discussion started: 31 March 2026

Erosion and dispersal processes drive vegetation trajectories in a highly erosive badland catchment

Caroline Le Bouteiller[1], Thomas De Almeida[1,2], Juliette Pellerano[1], Arthur Bayle[3,4], Philippe Choler[4], Laurent Borgniet[5], Hemanti Sharma[1], Sebastien Klotz[1]

[1]Institut des Geosciences de l'Environnement, INRAE, UGA, CNRS, IRD, Grenoble INP, Saint Martin d'Heres, 38400, France
[2]UMR 5600 Environnement Ville Société (EVS), CNRS, Lyon, France
[3]Climate Change Impacts and Risks in the Anthropocene (C-CIA), Institute for Environmental Sciences, University of Geneva, Geneva, Switzerland
[4]Univ. Grenoble Alpes, Univ. Savoie Mont Blanc, CNRS, LECA, Grenoble, France
[5] Univ. Grenoble Alpes, INRAE, LESSEM, St-Martin-d'Heres, France

Correspondence to: Caroline Le Bouteiller (caroline.le-bouteiller@inrae.fr)

Abstract. Badlands are among the most erosive places on earth, providing large sediments fluxes to rivers and oceans. In these environments, erosion is strongly controlled by vegetation, whose cover and composition both vary in space and time. Quantifying vegetation dynamics and their drivers is therefore essential to understand and predict badland erosion. Here, we use time series of high-resolution aerial and Landsat satellite imageries to reconstruct 40 years of vegetation change in a highly erosive badland catchment of French south-western Alps. Vegetation cover increased from 38.7% to 46.2% of the studied area), primarily through the colonization of bare surfaces by young pines. Spatial patterns of colonization and extinction are driven both by geomorphic factors, such as slope stability and local erosion rate, and by ecological factors, such as grain dispersal. Remotely sensed greening trends are correlated with climate, initial vegetation type and colonization intensity, suggesting that both climate changes and ecological succession are contributing to the greening of badlands. Quantifying these spatial and temporal trends reveals that vegetation dynamics are tightly coupled with erosion, as they both control and respond to erosion patterns.

1 Introduction

Erosion is a critical issue for human society. Hydric erosion threatens soils and agriculture (Pimentel, 2006). Sediment fluxes generate and amplify natural hazards (Badoux et al, 2014, Vasquez-Tarrio, 2024) and reduce hydropower capacity through reservoir infilling (Syvitsky, 2005). Suspended sediments affect water quality by reducing light and oxygen availability, degrading stream habitats and biodiversity (Billota and Brasier, 2008), and contributing to pollutant dispersion and transport (Herrero et al, 2018). Over longer timescales, mountain erosion and weathering contribute to the global carbon cycle, acting either as a source or a sink of atmospheric CO2 (Hilton and West 2021) with a tight link to climate evolution.

Erosion is strongly affected by vegetation through multiple processes. Vegetation reduces erosion by decreasing runoff (via rainfall interception, enhanced infiltration and soil surface roughness, e.g. Bochet et al, 2006) and by reinforcing soil cohesion

https://doi.org/10.5194/egusphere-2026-834
Preprint. Discussion started: 31 March 2026

(Gyssels et al, 2005, Lobmann et al, 2020), but it may also enhance soil production and creep (Richardson and Perron, 2019, Samonil et al, 2023). In the coming decades, erosion is expected to increase in many regions under climate and land use changes (IPPC 2019, Li and Fang, 2016, Nearing et al, 2004). At the same time, vegetation itself is responding to climate change. A climate-driven "greening" trend, i.e. increases over time in satellite-based vegetation indices, has been observed in many parts of the world (Nemani et al, 2003, Zhu et al, 2016; Berner et al. 2020) including mountains (Choler et al. 2021; Anderson et al. 2020). In the European Alps, this greening was attributed to treeline upward shift (Bayle et al. 2025a; Nicoud et al. 2025; Bayle et al. 2025b) and increases in low stature vegetation cover (Choler et al. 2025). This increasing vegetation cover has the potential to reduce erosion rates. Predicting erosion therefore requires understanding how the intertwined vegetation dynamics and geomorphic processes will respond to climate forcing (Eichel et al, 2023).

Our study focuses on badlands, i.e. steep, dissected landforms developed on weak sedimentary rocks. Badlands are widespread in the Mediterranean region (Nadal-Romero et al, 2021) and are key contributors to sediment and carbon fluxes to the Mediterranean Sea. For instance, badlands represent only 0.2% of the Rhone watershed area but contribute 14% of its total sediment export and 12% of the export of petrogenic particulate organic carbon to the sea (Copard et al, 2018). Predicting future badland erosion is therefore crucial for hazard mitigation, hydropower management, drinking-water quality, biodiversity conservation and restoration, and for improving climate models. This in turn requires understanding how vegetation control over badland erosion evolves through time.

Vegetation is generally sparse in badlands (Gallart et al, 2013). Steep slopes form a hostile environment for plants: individuals can be uprooted by extreme run-off, gully erosion or shallow landslides or buried under sediment deposits (Burylo et al, 2009, Guerrero-Campo et al, 1999). Moreover, where erosion rates exceed soil formation, soils are thin or absent, which further limit plant establishment and growth. However, where vegetation can persist, it strongly limits badland erosion (Carriere et al, 2020, Canton et al, 2001, Gallart et al, 2013) and promotes soil formation and stabilization (Erktan et al, 2016). Vegetation recolonization can thus decrease badland erosion, which could be potentially amplified by a positive feedback in which stabilized soils are more easily recolonized (Marston, 2010, Amundson et al, 2015). Vegetation patterns in badlands have been found to respond to topographic contrasts. In semi-arid badlands, Bochet et al (2009) observed that vegetation was water-limited and therefore concentrated on gentle North facing slopes. In contrary, in humid badlands, Nadal-Romero et al (2014) found denser vegetation cover and higher species richness on South-facing slopes, suggesting limitation by temperature or by enhanced erosion on the North-facing slopes. These studies, based on spatial vegetation and species richness patterns at single point in time, do not reveal whether the observed distributions are at equilibrium or still adjusting to climate or disturbance regimes nor how they may respond to future environmental changes.

The aim of this paper is (i) to quantify vegetation dynamic in a badland area in the south-eastern France and (ii) to identify the factors that control this dynamic. We hypothesise that badland vegetation dynamics could be driven by climatic factors such as temperature and precipitation, by erosion acting both directly (through sediment fluxes) and indirectly (through topography), and by ecological processes such as natural succession and dispersal. To test this hypothesis, we focus on the Laval badland

https://doi.org/10.5194/egusphere-2026-834
Preprint. Discussion started: 31 March 2026

catchment of Draix-Bleone critical zone observatory, where long-term climate, erosion and vegetation data are available (Klotz et al, 2023). We first map vegetation dynamic over the period 1982-2022 by combining historical Infra-Red (IR) aerial photographs with Landsat satellite imagery. We then relate the observed dynamic to climatic, geomorphic and ecological variables, to explain spatial and temporal patterns of vegetation dynamics in badlands.

2 Material and methods

2.1 Study site

This study was carried out in the badlands known as Terres Noires, in south-eastern France. These badlands are developed on Jurassic black marl outcrops, and are characterized by deeply incised gullies, high drainage density and intense weathering and erosion processes. As a result of heavy demographic pressure in the Middle Ages, the region suffered from severe erosion and flooding, before undergoing a policy of reforestation at the end of the 19th century. Some areas of the badlands were reforested with Austrian black pine, while others were left bare, with vegetation naturally re-establishing in the less steep areas (Vallauri et al, 2002).

The Draix-Bleone Critical Zone Observatory was setup in the early 1980s to study runoff and erosion processes in these badlands. A large dataset on meteorological forcing, runoff and sediment fluxes over the last 40 years is therefore available and geomorphic processes including weathering, erosion and sediment transport, are well documented (Klotz et al, 2023, Mathys et al, 2003, Rovera and Robert, 2003, Ariagno et al, 2023, Esteves et al, 2005, Descroix and Mathys, 2003). Erosion rates are among the highest recorded worldwide with an average of 15000t/km2/yr in the bare badlands, whereas comparison with neighbor reforested badlands have shown that sediment yield was reduced by a factor of 200. This reduction was mostly attributed to the reinforcement of soil cohesion by roots (Carriere et al, 2020).

Two areas in the badland zone of the observatory are defined for the present study (see Figure 1): The first is the Laval catchment, which is part of Draix-Bléone critical zone observatory (Klotz et al, 2023). This small catchment (0.86 km2) has a homogeneous lithology of black marls from the callovo-oxfordian and bathonian periods, and a badland morphology with high drainage density, steep slopes (mean slope of 0.58) and sparse vegetation cover. Elevation ranges from 850 to 1200 m. The vegetation includes grassland dominated by *Brachypodium pinnatum*, forested stands of pine trees (*Pinus sylvestris* and *Pinus nigra*) and deciduous trees (*Fagus sylvatica* and *Quercus pubescens*), and pioneer zones with a mixture of herbaceous (*Achnatherum calamagrostis*), shrubs (*Genista cinerea*, *Hippophae rhamoides*, *Amelanchier ovalis*) and trees (*Pinus nigra*). Vegetation is mainly associated with lower slopes and quaternary deposits that locally cover the ridges. Because the catchment is small compared to the resolution of Landsat images (30 m), an extended study area of 8 km2 was defined around the Laval catchment to ensure the robustness of Landsat-based analyses. This area exhibits the same lithology, morphology and elevation range (Figure 1). Vegetation in this area is no longer disturbed by land use, except for a few cultivated areas that are excluded for the analysis.

https://doi.org/10.5194/egusphere-2026-834
Preprint. Discussion started: 31 March 2026

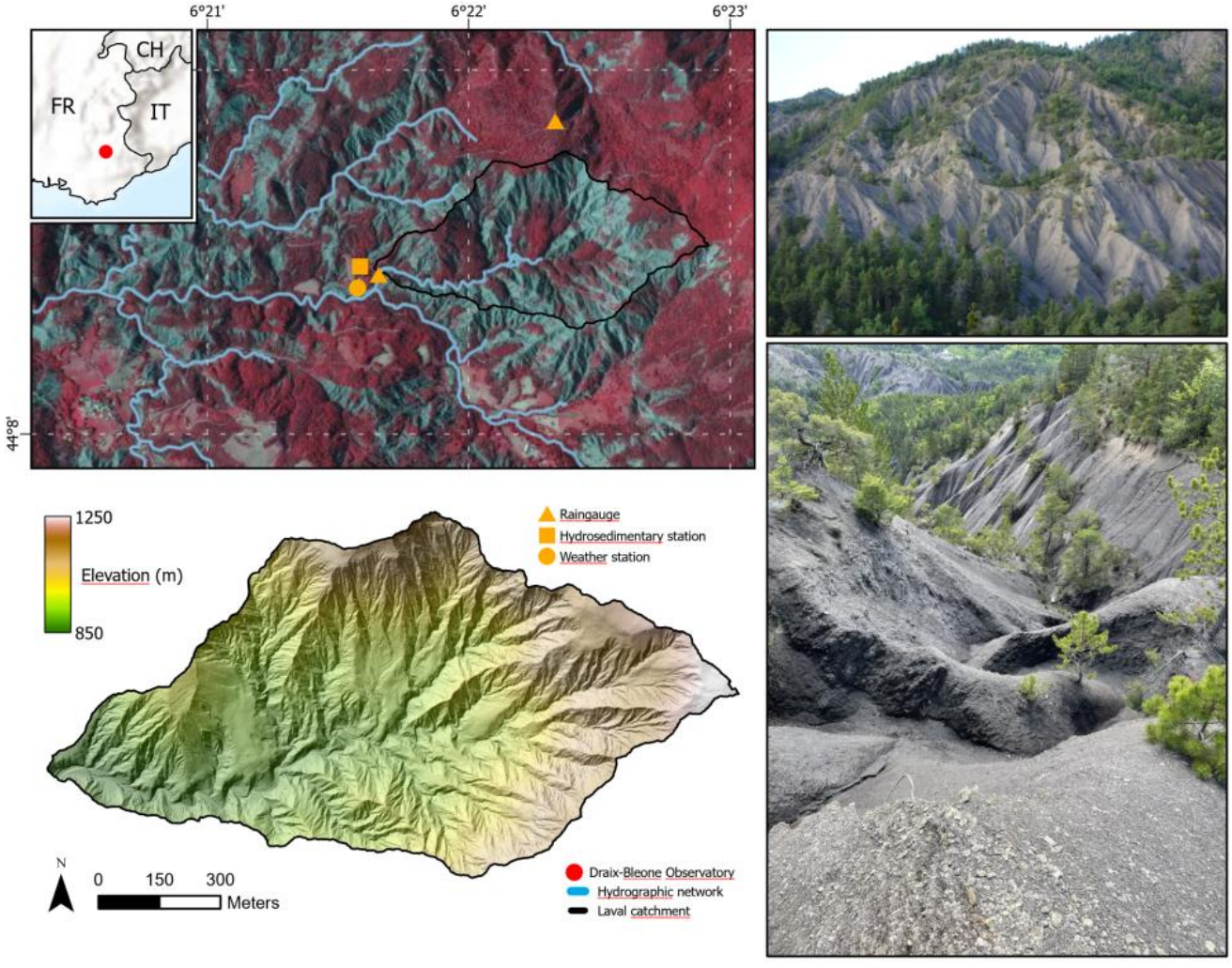

Figure 1: Location of Draix-Bleone Observatory,Laval catchment, and monitoring stations. Background aerial phot, shaded relief and hydrographic data from IGN BDortho, BDalti and BDtopo (2024). Photographs from Laval catchment showing pine colonization on badland slopes.

The climate is characteristic of a Mediterranean mountain region with two rain periods in spring and autumn, winter frost and intense summer storms that may give rise to flash floods. Mean annual rainfall is 919 mm at the Laval rain gauge over the period 1985-2022 and mean annual temperature is 9.9°C at the Plateau station over the period 2001-2022 (Klotz et al, 2023).

2.2 Time series of temperature, precipitation and sediment exports

Temperature data is measured at Draix weather station since 2001. To reconstruct a mean annual temperature record prior to this period, we use daily temperature data from Meteo France weather station located at Marcoux, 6 km away and 150m lower than Draix weather station. We quantify a systematic relationship between the two sites by fitting a linear regression on monthly temperatures over the overlapping period 2001-2005 ($R2 = 0.997$) and use this relation to reconstruct monthly

https://doi.org/10.5194/egusphere-2026-834
Preprint. Discussion started: 31 March 2026

temperature at Draix between 1984 and 2001. We then compute a mean annual temperature based on these monthly temperatures.

High resolution rainfall data is available from Draix-Bleone observatory data since 1983 (Klotz et al 2023). The Laval rain gauge data is used, and complemented by the data from the nearby Pompe rain gauge when needed. Annual precipitation is computed by cumulating rainfall over each year. Snow is infrequent in this site, and when it occurs, the rain gauge is heated therefore it records the equivalent volume of melted water.

Sediment fluxes both as bedload and suspension are recorded at the Laval hydrosedimentary station, using high-frequency turbidimeters, automatic samplers, and topographic surveys of a sediment trap (details in Klotz et al, 2023). This allows computing event-scale exported sediment volumes.

2.3 Aerial photographies

Aerial Infra Red and color photographies from IGN (Institut Geographic National, https://remonterletemps.ign.fr) are available for dates 1982, 1994, 2012, 2015 and 2021. Photographies from 2012, 2015 and 2021 were already orthorectified by IGN (BDortho IRC, IGN). We orthorectified the 1982 and 1994 photos using the Structure-from-Motion (SfM) method (Knuth et al, 2023) with Agisoft Metashape software (version 1.7.3). The horizontal error computed over 10 well distributed ground control points was less than 2m. All the images were then adjusted to a common resolution of 0.5 m.

Aerial images were then classified based on a combination of Near Infra Red (NIR), red and green bands, Normalized Difference Vegetation Index (NDVI), computed using the red and NIR bands, and an energy texture index (Haralick, 1979). The following five classes were identified: bare soil, deciduous forest, pine forest, grassland, and shade. The shade class corresponds to some steep slopes that are not enough illuminated in the photo to define the vegetation cover, even visually, as well as shadows from objects above ground like trees. A pixel-based supervised classification was run using a random forest algorithm with the software OTBtoolbox (Grizonnet et al, 2017). The classification accuracy was verified over 1,500 to 3,000 points and was higher than 97% for all images. After classification, the shade class represented less than 2% of the surface for all images, except for 2012 image where it represented 20%. Finally, the vegetation maps obtained from the classification were smoothed using an expansion/contraction algorithm (BoundaryClean ARCGIS) to remove small-scale interface variability. First, we compare vegetation maps between each pair of dates to map pixel-based transitions. Secondly, we group the three types of vegetation into a single class to create binary images (vegetated vs. bare). Comparing these binary images between two dates allows capturing where vegetation has replaced bare ground and where bare ground has replaced vegetation.

2.4 Satellite images

We utilized all Tier 1 data available over our study site from 1984 to 2022 for the months June, July, August and September in Landsat Collection 2 provided by the U.S. Geological Survey (USGS) and hosted on Google Earth Engine (GEE). The tier 1 data products analyzed include surface reflectance from Landsat 5 Thematic Mapper (TM), Landsat 7 Enhanced Thematic Mapper + (ETM+) and Landsat 8 Operational Land Imager (OLI). We exclusively chose images with an average cloud cover

https://doi.org/10.5194/egusphere-2026-834
Preprint. Discussion started: 31 March 2026

of less than 80 %, as scenes with high cloud cover can compromise the accuracy of geometric calibration. The C Version of Function of Mask (CFmask) was applied to categorize each pixel as clear (land/water), snow, cloud, adjacent to cloud, or cloud shadow (Zhu et al., 2015; Zhu & Woodcock, 2012). Pixels affected by snow, cloud, adjacent to cloud or cloud shadow were excluded from the analysis. Berner et al., (2020) identified systematic radiometric discrepancies among Landsat 5 TM, 7 ETM+, and 8 OLI satellites. We corrected for it using cross-sensor calibration coefficients from Choler et al. (2025).

We computed NDVI using cross-sensor calibrated Red and NIR bands and computed the annual maximum during the growing season. (Berner et al., 2020) demonstrated that NDVImax estimates are dependent on the number of observations during the growing season. (Bayle et al., 2024) showed that, because Landsat observations increase over the time series, the dependence of NDVImax on sampling frequency can lead to an overestimation of greening trends. (Berner et al., 2023) showed that this sampling bias can be partially corrected by modelling phenology on a pixel-by-pixel basis and adjusting the estimates of NDVImax based on mean phenology. Hence, we applied phenological modelling to adjust NDVI values before computing NDVImax. We relied on the Harmonic Analysis of Time Series (HANTS) reconstruction method as used by (Choler et al., 2025). This procedure was only applied on NDVI observations with values higher than 0.15 to eliminate unvegetated pixels as the correction relies on phenological modelling. The complete procedure, relying on state-of-the-art methods allowed us to derive a robust annual NDVImax series for our study site. Greening is defined as the slope of the NDVImax series. We determined slope estimates pixel-wise using a non-parametric Theil-Sen slope estimator (Sen, 1968) as implemented in GEE. Greening trends at 30m resolution were then combined with high-resolution vegetation maps to obtain a detailed information of vegetation types within each Landsat pixel. When more than 90% of the Landsat pixel is of the same vegetation type over the whole study period, this pixel is defined as a “pure” Landsat pixel, which means that it is representative of one vegetation type. We also define a colonisation intensity indicator as the percentage of the surface in each Landsat pixel that transitioned from bare to vegetated over the 40-year study period.

2.5 LiDAR data

High-resolution LiDAR data over Draix badlands is available in 2015 and 2021. The first LiDAR point cloud was acquired in 2015 from helicopter by Sintegra (private company specialized in topography), with a resolution of 160 pts/m2. Filtering for vegetation was run by the producer and the remaining soil surface point cloud has a resolution of 40 pts/m2. This point cloud was used to create a 50 cm resolution discrete elevation model (DEM) (Le Bouteiller et al, 2023). Local slopes, aspect, elevation, and drainage areas are computed using standard GIS tools using this DEM. Secondly, we used the Lidar dataset acquired in 2021 from plane by IGN (IGN, 2024), which has a resolution of 10 pts/m2. This dataset was classified by the producer into several vegetation classes and soil surface. In this study, we only use LiDAR data to assess local erosion therefore we filtered out vegetation in order to work on the soil surface.

Both LiDAR point clouds were already georeferenced by their producers, but we realigned them to get a finer adjustment using Cloudcompare software and the ICP algorithm (Besl and McKay, 1992). Because flat non-eroding zones are rare and not well spatially distributed in this catchment, we chose to use the whole point clouds to search for the best alignment. Using the full

https://doi.org/10.5194/egusphere-2026-834
Preprint. Discussion started: 31 March 2026

point clouds for alignment assumes macroscopically uniform erosion across the study area, with no directional trend. This method yields relative, rather than absolute, erosion rates, and thus requires recalibration using known exported volumes to obtain absolute values. After alignment, we computed the vertical distance between the point clouds using the C2M algorithm from Cloudcompare. Based on the sediment export records at the Laval station, 89000 tons of sediment were exported between the two LiDAR surveys. Using an average regolith density of 1.55 (Bechet et al, 2016, Mallet et al, 2020, Ariagno et al, 2023), this sediment export corresponds to a mean ablation of 0.068 m over the period. We then corrected the distance obtained from C2M algorithm by translating vertically one point cloud relatively to the other, in order to match this value. After this correction, we checked the distance obtained over a few non-eroding zones (cabin roofs) and found that it averaged to 0.002 ± 0.033 m, which provides an estimate of the distance uncertainty. Finally, the distance associated with the point cloud was transformed into a 0.5 m-resolution raster and divided by the number of years to obtain a map of annual erosion rates. Two areas were excluded from the erosion analysis: the main channel, where bed elevation fluctuates seasonally by more than 0.5 m due to sediment storage and entrainment processes, and the sediment trap.

2.6 Statistical analyses

First, analysis aims at explaining vegetation changes over the 40-year period. We investigated the role of slope, elevation, drainage area, aspect, local erosion rate, and vicinity of existing vegetation, as possible explanatory factors for colonization and extinction... The vicinity of existing vegetation is evaluated by counting the number of vegetated pixels in a 5x5 pixel window at the date before the transition. As a first approach to search for factors of colonisation, we compared the characteristics of pixels that undergone a transition from bare ground to vegetation to those of pixels that remained unvegetated. Similarly, to search for factors of extinction, we compare the characteristics of pixels that undergone a transition from vegetated to baren to those of pixels that remained vegetated. We use a Wilcoxon test to assess if the differences between transitioning and non-transitioning pixels are significant. Secondly, for each potential explanatory factor, we binned the data into classes and computed empirical colonization probabilities as the observed proportion of pixels that become vegetated among the pixels that were initially baren in each class. We similarly defined empirical extinction probabilities as the proportion of pixels that became bare ground among the pixels that were initially vegetated, within each class. This permits us to analyse how the colonisation and extinction probabilities depend on the value of each factor.

We also performed statistical analysis on the spatial and temporal trends of greening. To search for factors of spatial heterogeneity in greening, we compare greening patterns with initial NDVI value, type of vegetation and colonisation intensity. To search for factors explaining temporal trends, we compare annual maximum NDVI time series with annual precipitation, and mean annual temperature (MAT) using standard Pearson correlation analysis.

https://doi.org/10.5194/egusphere-2026-834
Preprint. Discussion started: 31 March 2026

3 Results

3.1 Vegetation evolution over 40 years

Vegetation maps are produced for dates 1982, 1994, 2012, 2015 and 2021 (Figure 3). Comparing these maps indicates a general colonization trend, with a total vegetation cover that increases from 38.7% to 46.2% over the study period. Bare ground diminishes from 62.3% to 53.8% as it transitions towards grassland and pine forest, and grasslands is reduced from 16% to 7.7% and is mostly replaced by pine forest. In total, the largest change is the pine forest that increases from 17.3% to 34.4%. The amount of deciduous forest stays stable at around 4-5%.

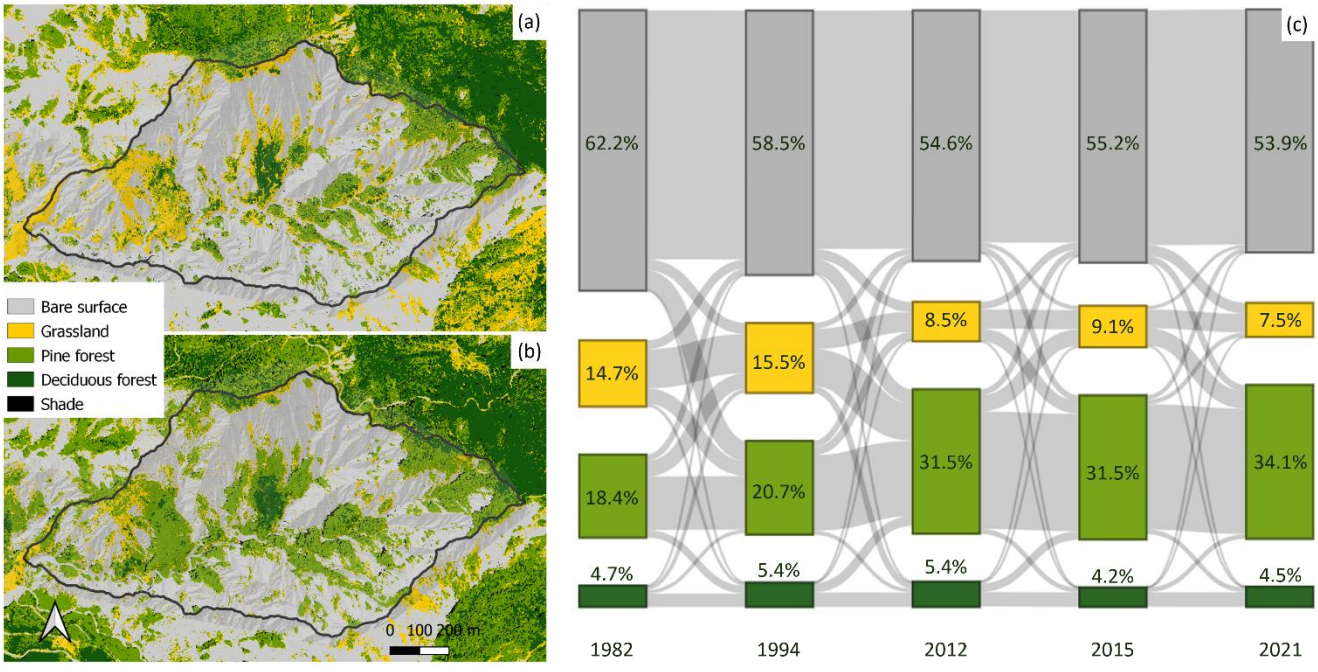

Figure 2: Vegetation classification for 1982 (a) and 2021 (b), and pixel-based evolution of vegetation types over the study period (c). Black line indicates the Laval catchment.

3.2 Greening trend

Maximum annual NDVI has generally increased over the study period (Fig. 6), although with marked spatial heterogeneity. In the extended study area, a few zones show browning trends. These zones are identified either as cultivated areas or as a clear cut and are later removed from the analysis. Within the Laval catchment, negative trends are mainly observed in the steep headwaters and in a localized zone of the left bank where a landslide occurred in 1998 (Garel et al, 2012). The highest greening values observed in the study area correspond to an increase of the NDVI of 0.0078 NDVI/year over the period (0.0059 NDVI/year in the Laval catchment), and the lowest values correspond to -0.0028 NDVI/ year.

https://doi.org/10.5194/egusphere-2026-834
Preprint. Discussion started: 31 March 2026

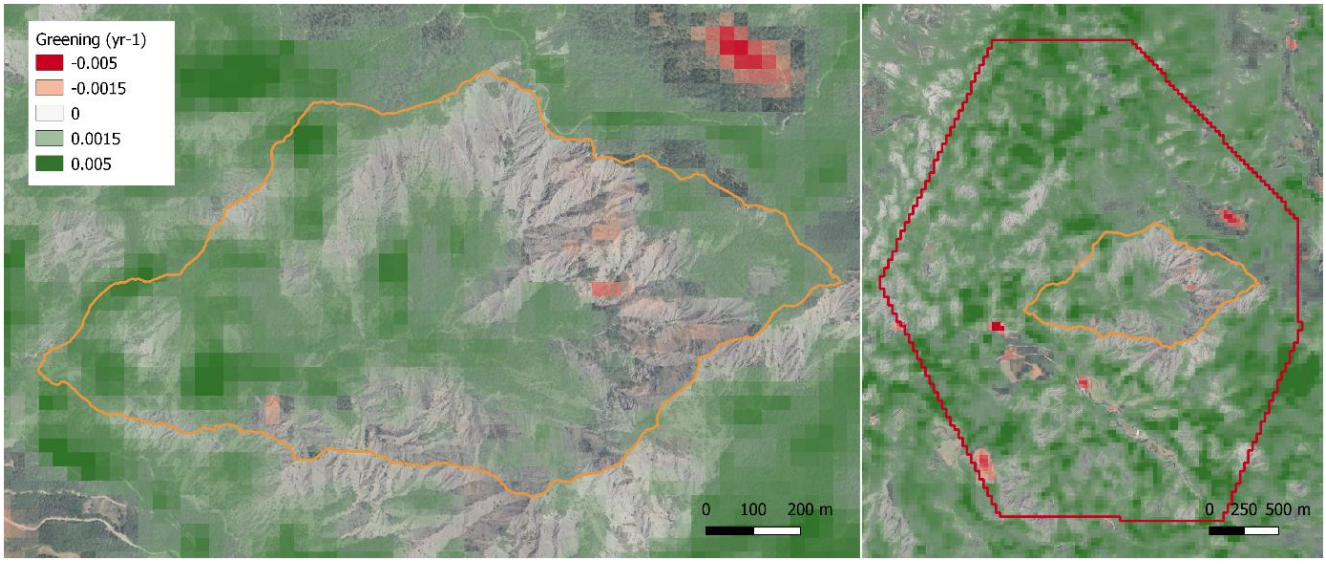

Figure 3: Map of greening trend over the Laval catchment and the extended studied area. Greening is expressed as a unit change in NDVI index per year. The red areas outside of the Laval catchment correspond to clearcutting and cropland that have been removed from the analysis. Background aerial photo from IGN BDOrtho

We first analyse the spatial variability of greening as a function of the initial NDVI. The grey transparent dots in Fig. 7a correspond to Landsat pixels (30m x 30m) and reveal a bell-shape relationship between initial NDVI and greening: pixels with very low or very high initial NDVI tend to show little greening, while those with intermediate initial NDVI exhibit the strongest positive trends. Among these, the pixels identified as "pure" (i.e. composed almost entirely of a single land cover type) show contrasted behaviors. Bare soil pixels has low initial NDVI and very low greening values (0.0005 NDVI/year), grassland and pine forest share similar intermediate initial NDVI values but pine forest shows much higher greening values than grassland (0.0035 vs 0.0008 NDVI/year). Deciduous forest pixels have the highest initial NDVI but only a moderate greening trend (0.0014 NDVI/year). Finally, when considering the fraction of the pixel surface that went through a transition from bare to vegetated (Figure 7b), the pixels with the most transitions correspond to high greening values with low to intermediate initial NDVI. High greening values are therefore obtained in two main cases: pure pixels of pine forest, and transitioning pixels.

https://doi.org/10.5194/egusphere-2026-834
Preprint. Discussion started: 31 March 2026

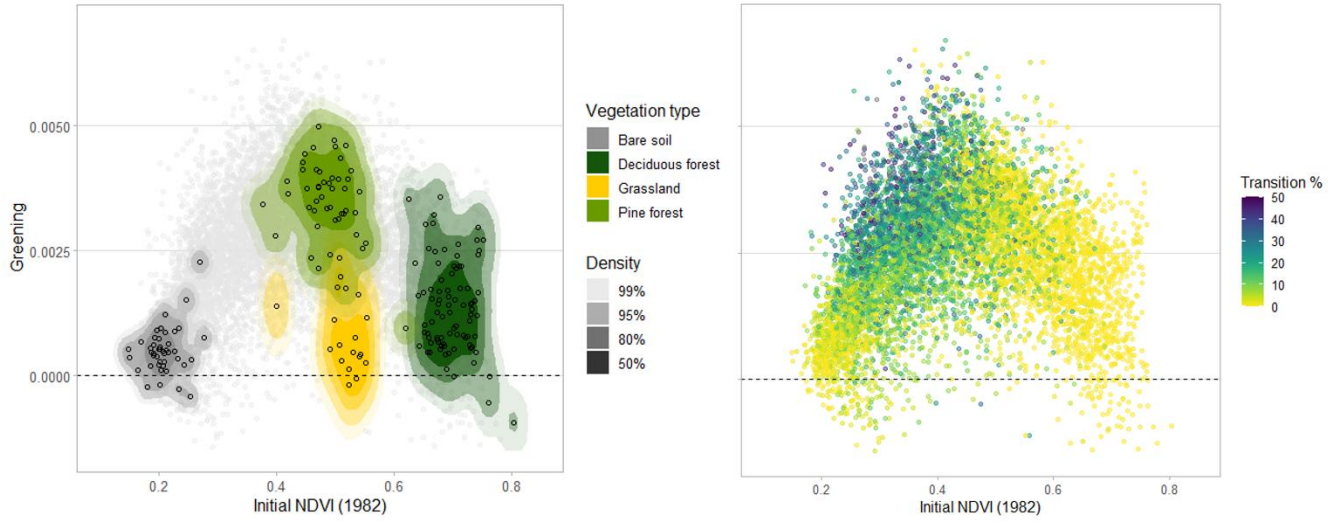

Figure 4: Greening as a function of initial NDVI. (a) pure pixels are colored according to land cover type and (b) all pixels are colored according to the percentage of their surface that transitioned from bare to vegetated over the period.

As already suggested in Fig. 7a, greening trend clearly depends on the type of vegetation. We therefore examine in more detail the temporal dynamic of NDVImax for each vegetation type, using only the "pure" pixels, and its relation to climate variables. Correlations between the temporal dynamic of NDVImax, averaged across all pure pixels of each type, and climatic variables from Draix-Bleone observatory, are reported in Table 1. For trees (both pine and deciduous forest), there are significant positive correlations between mean annual temperature and NDVI and negative correlations between the annual number of frost days and NDVI, but no significant trend with annual precipitation. On the contrary, grassland NDVI correlates significantly with annual precipitation and the annual number of frost days.

Table 1: Pearson correlations between annual maximum NDVI for each vegetation type and climate variables. Significance indicated in parenthesis (* means p-value <0.05, ** means p-value<0.01 and * means p-value <0.001)**

	Annual precipitation (mm)	Mean annual temperature (°C)	Annual number of frost days
Annual maximum NDVI - Grassland	0.4 (*)	0.0	-0.31 (*)
Annual maximum NDVI – Pine forest	0.25	0.58 (***)	-0.49 (***)
Annual maximum NDVI – Deciduous forest	0.10	0.26 (**)	-0.36 (**)

https://doi.org/10.5194/egusphere-2026-834
Preprint. Discussion started: 31 March 2026

3.3 Colonisation and extinction

Vegetation transitions are computed from binary maps and represented in Fig. 4. Vegetation colonization and extinction do not happen randomly over the catchment but appears to be spatially organized with hotspots of colonisation and extinction across the catchment. We find significant differences between transition types (p-value < 1e-4) for all tested factors, suggesting that they all have have an impact on vegetation trajectories.

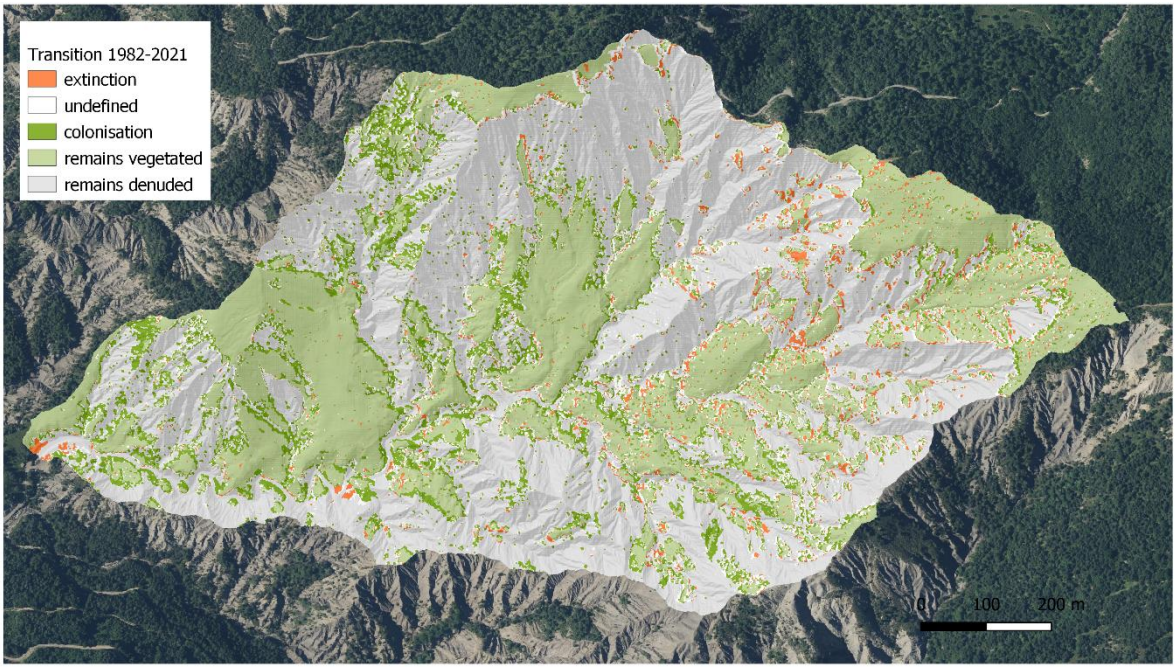

Figure 5: Evolution of the distribution of vegetation types over the study period

Figure 5 shows the colonization and extinction empirical probabilities computed as a function of local variables. First, colonization is controlled by slope, with more transitions at low slopes, and particularly at slopes between 20 and 50%, where colonization probability reaches a maximum value of 0.5. On the contrary, colonization is infrequent at slopes close to zero, and at slopes higher than 100%. Extinction shows the opposite trend, with extinction probability less than 0.1 for slopes lower than 80% and more than 0.5 for slopes higher than 300%. Secondly, colonization increases when the neighborhood is more vegetated. When the neighborhood is bare, the colonization probability is as low as 0.12 then reaches 0.5 when 4% of the neighborhood (i.e. one pixel in a 5x5 window) is already vegetated. On the contrary, extinction probability decreases as the neighborhood is more vegetated, and reaches 0.02 for points that are entirely surrounded by vegetation. Third, colonization is more frequent for the lowest and highest elevations in the catchment than for intermediate elevations (950-1150 m a.s.l.). It shows a particularly sharp increase in the highest elevations (>1230 m) where all bare surface were colonized. Extinction shows an opposite trend with more frequent extinction at intermediate elevations (1000-1150m) than at low and high

https://doi.org/10.5194/egusphere-2026-834
Preprint. Discussion started: 31 March 2026

elevations. Fourth, both colonization and extinction are rather constant with drainage area, except at the highest drainage a reas (> 2000 m2), that correspond to the main channel network. In this range, colonization probability decreases whereas extinctio n probability increases as high as 0.8. Fifth, colonization probability is positive when erosion rate is negative, i.e. in depo sitional environments, and decreases towards zero for positive erosion rates. Extinction probability follows the opposite trend. F inally, both colonization and extinction appear to be slightly more frequent for northern aspect than southern aspect. Mean colonization probability is 0.2 in the northern half (W to NE) versus 0.16 in the southern half (E to SW), and mean extinction probability is 0.11 in the northern quarter (NW to NE) versus 0.06 in the eastern, southern and western quarters.

Correlation tests between all explanatory variables in the initially bare subsample (respectively initially vegetated) indica te a correlation of 0.24 (respectively 0.23) between slope and elevation and correlations lower than 0.15 between all other variab les. When classifying elevation and slope data, high elevation (more than 1230m) appears to be associated with low slopes (lower than 50%). Similarly, slopes between 0 and 10% are strongly associated with high drainage areas and mostly corresponds to the channels.

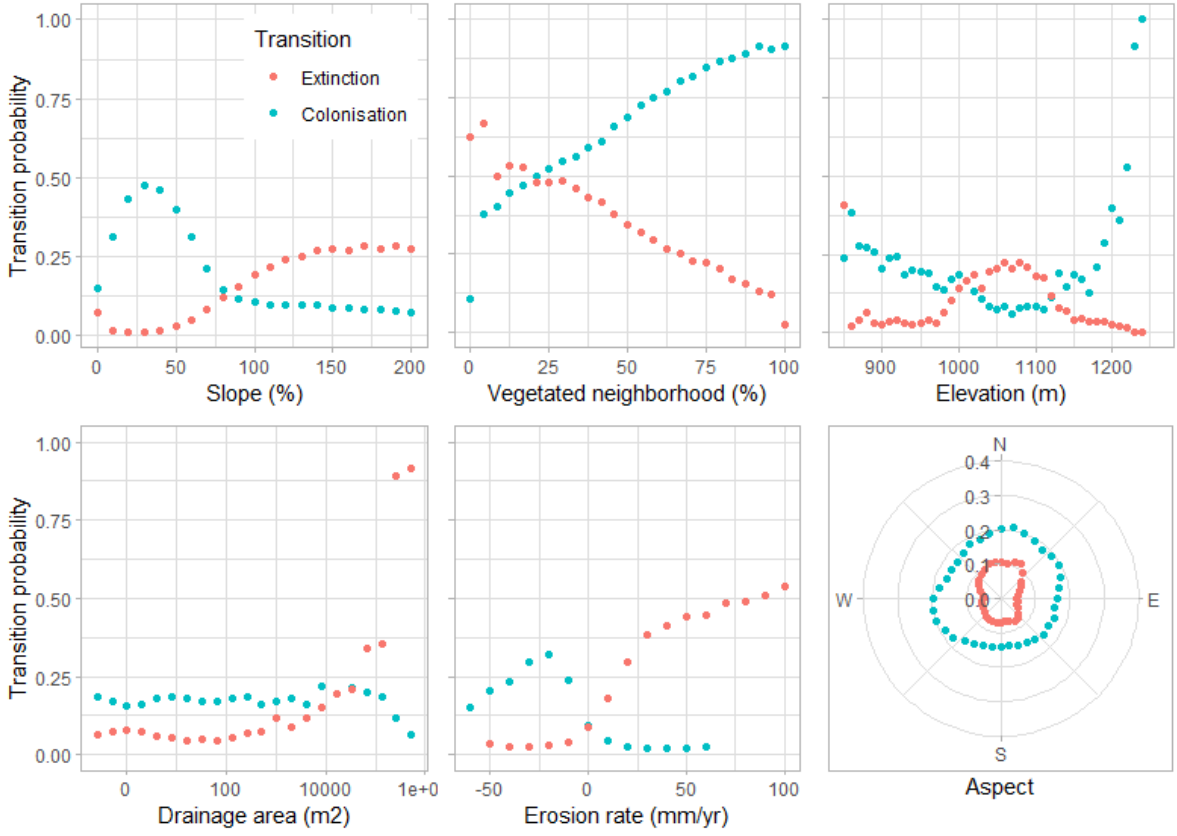

Figure 6: Colonization and extinction probability as a function of local variables: slope, neighborhood vegetation cover, elevation, drainage area, local erosion rate and aspect. Transition probabilities are computing over the period 1982-2021 for all variables except for (e) where they are computing over the period 2015-2021.

https://doi.org/10.5194/egusphere-2026-834
Preprint. Discussion started: 31 March 2026

4 Discussion

4.1 What controls temporal trends of vegetation dynamics?

Both time series of aerial and satellite imagery are evidencing increased vegetation cover over the last decades in the Laval catchment area, which aligns with observed large-scale greening in mountainous regions (Choler et al. 2021; Anderson et al. 2020). Our analysis of aerial photographs reveals expansion of vegetated areas, both by trees and grasses, which is also reflected in the Landsat imageries. In addition, the overall greening trend, also observed in pure vegetation pixels, suggests that vegetation not only expands spatially but also exhibits enhanced growth. These dynamics are consistent with greening trends reported in other mountainous and high-latitude regions worldwide (Zhu et al., 2016; Carlson et al., 2017; Liu et al., 2019), which are often attributed to climate warming, particularly in mountain areas where warming rates are high (Pepin et al., 2015; Lucht et al., 2002; Dumont et al. 2025). Higher temperatures tend to advance snowmelt and extend the growing season (Choler et al. 2025). At our study site, snow is infrequent and, when present, melts quickly, so snowmelt is unlikely to limit vegetation growth. Instead, winter frost may play a key limiting role, as suggested by the negative correlations between NDVI and the annual number of frost days (Table 1). Rising temperatures are associated with shorter freezing periods, which likely favour vegetation growth and colonisation by both trees and herbaceous species. A decrease in spring frost events occurring after germination may help explain the higher success of recent colonisation.

The colonisation dynamics we observe are also similar to those reported in other badland areas, where they have been attributed to a decline in human activity (Torri et al., 2018). For instance, the Italian "biancana" badlands of Val d'Orcia were historically associated with human disturbance through overgrazing, erosion along animal tracks, and burning, and are now retreating due to rural abandonment (Torri et al., 2013; Bayle et al. 2025b). The Draix badlands have experienced little recent human influence (apart from extensive grazing on grassland interfluves, affecting less than 1% of the Laval area). However, this region of the pre-Alps was more densely populated in the Middle Ages, which likely increased grazing pressure and firewood collection (e.g. Gamba et al., 2024). It is therefore possible that vegetation recolonisation is also a long-term response to the reduction in anthropogenic pressure, although this reduction began long before the period we analyse here. Consequently, it is not possible to attribute current vegetation dynamics with certainty to rising temperatures and reduced frost alone. Attribution studies using process-based models to compare vegetation responses under stationary versus time-varying climate conditions would be needed to test this hypothesis. Such models, however, require a detailed process-based understanding of how different plant communities respond both to warming and to the abandonment of traditional land-use practices, which is not yet available.

4.2 What controls spatial trends in vegetation dynamics?

Locally, vegetation dynamics appear to be related to slope, which is a critical factor for both recolonization and extinction. At very low slopes (less than 10%), colonization is reduced whereas extinction is increased. Such low slopes correspond to the channel network, where water and sediment fluxes are concentrated and do not permit plant colonization. Colonization and extinction probabilities observed at low slopes are also consistent with the trends seen in areas with the highest drainage areas.

https://doi.org/10.5194/egusphere-2026-834
Preprint. Discussion started: 31 March 2026

Beyond this, there is a clear slope control on both colonization and extinction. Colonization probability peaks at a slope of ~30-40% and then decreases towards a non-zero but consistently low plateau. In contrast, extinction probability is close to zero at low slopes and increases with slope towards a higher plateau (Figure 5a). We define a critical slope as the slope where extinction probability first exceeds colonisation probability, meaning that, in the long term, vegetation is more likely to decline than expand on slopes steeper than this value. We find a critical slope of 90% (42°). Moreover, colonization is associated with negative erosion rates (i.e. deposition), whereas extinction is associated with positive erosion rates (Figure 5e). The slope threshold therefore corresponds to a stability threshold for unconsolidated material, above which it can start to move. The impact of slope on vegetation dynamics thus strongly reflects the influence of erosive processes. Plants rarely establish or persist on slopes where erosion regularly removes several millimetres of material.

Erosion can affect ecological process at different stages. Early in colonization, seeds may be removed from steep slopes by runoff (Cerda and Garcia-Fayos, 2002). After establishment, erosion can uproot young or mature individuals (Burylo et al, 2009, Lee et al, 2022) and, more generally, prevent the accumulation of litter and nutrients critical to plants (Gharamani et al, 2011). As our colonization measurements are integrated over several years, it is not possible to know at which stage erosion is most limiting, but it is reasonable to assume that young individuals with shallow roots are more sensitive to uprooting than older ones (Crouzy et al, 204). A finer temporal resolution for vegetation cover and erosion would be needed to relate disturbance frequency on steep slopes to colonization and extinction events at different stages of plant establishment and development.

The slope threshold value found here is lower than previously reported values for other badlands. Nadal-Romero et al (2014) observed a slope threshold for plant cover of 44° on North facing and 55° on south-facing slopes, whereas Bochet et al, (2009) found thresholds of 63 and 41° on South-facing and North-facing slopes, respectively. Note, however, that both studies analysed existing plant cover rather than dynamic pattern of colonization. In those sites, aspect contrasts were explained either by increased weathering and erosion intensity on North-facing slopes in humid badlands (Nadal-Romero et al, 2014) or by increased water stress on the South-facing slopes in a semi-arid site (Bochet et al, 2009). Our data shows slightly lower critical slopes on the SE aspect (39°) than NW aspect (45°), suggesting that water stress could modulate the competition between colonisation and extinction, although much less intensely than in the semi-arid badlands studied by Bochet et al (2009).

Vegetation recolonization is also strongly related to vegetation neighbourhood. Because we measure colonization from aerial images, we cannot rule out the possibility that part of the measured recolonization corresponds to the widening of tree crown, without the establishment of new individuals. However, field visits with tree coring clearly showed there were new individuals in the areas identified as recolonized from aerial images (unpublished data). The observed neighborhood dependency therefore suggests that colonization is controlled by seed dispersal processes. We tested different neighbourhood sizes and found that colonization probability was reduced to less than 2% when there was no vegetation within a radius of 10 meters. Debain et al (2007) estimated mean dispersal distances for *Pinus nigra* on a limestone plateau and found a mean dispersal distance of 8.5m for frequent, short-distance dispersal and 40 m for infrequent events associated with extreme winds. Our observations therefore suggest that, in Draix badlands, pine colonization is mostly controlled by short-distance dispersal. Nevertheless, in our dataset

https://doi.org/10.5194/egusphere-2026-834
Preprint. Discussion started: 31 March 2026

we did detect some very rare colonization events far (up to 50m) from where vegetation was already present in 1982, indicating that long-distance dispersal processes exist but are very infrequent. Because of the widespread runoff-generated erosion in this catchment, we may hypothesize that runoff and erosion could contribute to such long-distance dispersion. The data presented here could help test this hypothesis in a future study.

More surprisingly, in our dataset, extinction also appears to be related to neighbourhood (Figure 5b), with more extinction occurring for vegetation surrounded by bare soil. One possible explanation would be the existence of positive interactions between neighbouring trees that reduce environmental stresses. For instance, since our temporal analysis suggests that vegetation is affected by frost, a vegetated neighbourhood may protect a tree by dampening air temperature variations within the canopy (Haesen et al, 2021, De Frenne et al, 2019). However, because our quantification of extinction integrates several years, it is also possible that extinction occurs independently of the neighbourhood, but that recolonization follows quickly where a largely vegetated neighbourhood makes it likely, which would result in the observed trend for extinction. A smaller scale monitoring of extinction events would be necessary to conclude on this aspect.

Our dataset shows no strong impact of aspect on either colonization or extinction. In many places around the world, aspect contrast are observed both in existing vegetation structure and diversity (Badano et al, 2005, Gallardo-Cruz et al, 2009) and in greening trends (Choler et al. 2021; Yin et al, 2023). This contrast is often explained by differences in solar radiation, which would result either in a more favourable south-facing aspect when vegetation is temperature-limited at high latitudes or elevations, or in a more favourable north-facing aspect where vegetation is water-limited at lower latitudes and elevations (Pelletier et al, 2021). Here, initial vegetation in 1982 is slightly unbalanced: North-East aspects (E, NE, N and NW) have an average vegetation cover of 18%, while South-West aspects have an average vegetation cover of 26%. This could suggest that water limitation for vegetation in sun-facing slopes is less a problem than temperature limitation on shady slopes, but it could also be related to the fact that in this catchment, north-facing slopes tend to be steeper and hence more exposed to erosion than south-facing slopes. In any case, our colonization and extinction data do not exhibit strong aspect dependency, suggesting that the trade-off between water limitation and temperature limitation is not the main driver for vegetation dynamics here.

We also observe that colonization and extinction vary with elevation: however this trend is mainly due to correlation between high elevations and low slopes, which leads to higher colonization rates and lower extinction rates.

4.3 Consequences for the coupled system of vegetation and erosion

Our findings indicate that vegetation colonization is limited both by erosion and by dispersal. This has important implications for the coupled system of vegetation and erosion. From a biodiversity point of view, steep slopes appear to act as a barrier to vegetation, potentially disconnecting the vegetation on gently sloping ridges from that in floodplains. If hillslopes are longer than the typical dispersal distance of the main colonising species and steep enough to prevent establishment, we should expect genetically different populations on ridges and floodplains. Such a barrier effect has been observed, for instance, by Reuber et al, (2024), who found that steep slopes prevented mixing and drove genetic subdivision between rodent populations.

https://doi.org/10.5194/egusphere-2026-834
Preprint. Discussion started: 31 March 2026

Conversely, steep slopes could also contribute to long distance dispersal through overland flow and soil flux (Thomson and Katul, 2009, Ohsawa et al, 2007), although we have not clearly detected such a systematic pattern in our dataset.

Over longer timescales, landscape evolution modelling studies have shown that vegetated catchments tend to develop steeper equilibrium topography because vegetation slows their erosive response to tectonic uplift (Istanbulluoglu and Bras, 2005, Richardson et al, 2020). Since slopes cannot steepen indefinitely, they eventually become unstable and fail by landsliding, which also removes existing vegetation. If colonization is strongly limited on steep slopes, bare soil remains exposed and erosion increases, which should, in the long-term, reduce slopes and eventually allow colonization again (Fig. 8). Even under constant climatic and tectonic forcing, this steepness limitation on colonization would therefore prevent the system from reaching a long-term topographic steady state. Instead, it would oscillate between a barren state with high erosion and decreasing relief, and a vegetated state with low erosion and increasing relief. While many studies have underlined how climatic changes can trigger shifts to new equilibrium in coupled erosion/vegetation system (Sharma et al, 2021, Yetemen et al, 2019), our results suggest that the intrinsic characteristics of vegetation dynamics alone can generate such instability. This has important implications for how we interpret present-day landforms and vegetation patterns.

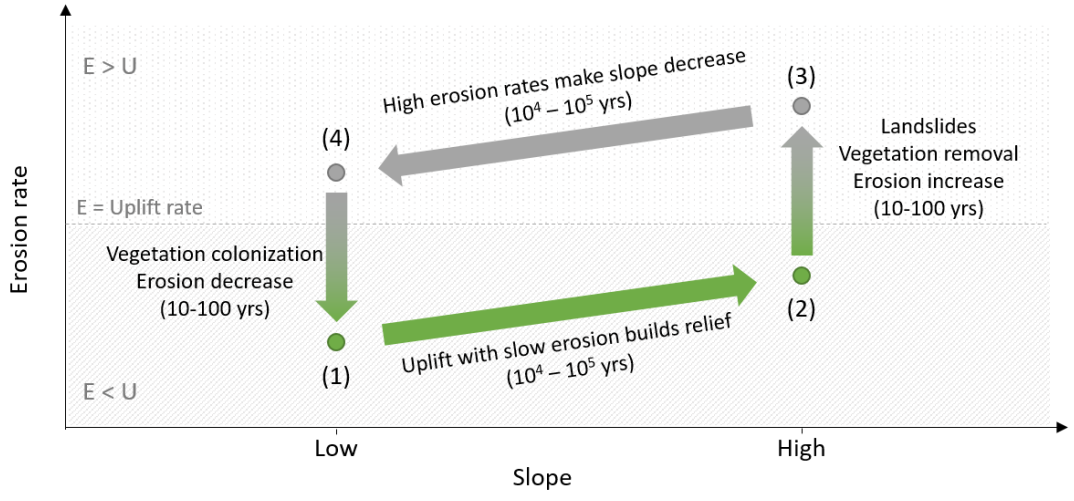

Figure 7: Cyclic evolution of coupled vegetation and topographic slope driven by tectonic uplift. (1) Vegetated cover and low slopes, low erosion rates. (2) Slope increases since uplift is faster than erosion, until it reaches a threshold for lanslide initiation (3) Landslides remove vegetation and erosion increases. (4) Slope decreases since erosion is faster than uplift until it is low enough to allow for recolonization.

Based on our findings, what can we expect for these badland catchments in the future? In the short-term, we expect colonization to continue, driven by climate warming and/or natural succession. In the long-term, several trends may occur. Mediterranean regions are expected to experience more intense rainfall (Zittis et al, 2021), which could accelerate erosion and limit recolonization. This could accentuate the contrasts between bare zones with accelerating erosion and vegetated zones with accelerating greening. Moreover, even if water limitation does not currently appear to constrain vegetation in these badlands, it may become important in the future and induce new vegetation patterns related to aspect or hillslope position (Famiglietti et

https://doi.org/10.5194/egusphere-2026-834
Preprint. Discussion started: 31 March 2026

al, 1998), or weaken oak and beech deciduous forests in favour of more drought tolerant species (Walde et al, 2026, Mas et al, 2024). Temperature warming is also expected to reduce frost-weathering intensity, slowing down regolith production and possibly erosion (Ariagno et al, 2022, Nadal-Romero et al, 2021), which would also favor recolonization. On even longer timescales, tectonic uplift is negligible compared to erosion in these catchments, meaning that the relief is overall flattening. Based on current erosion rates, the mean slopes of the Laval catchment would, for instance, be reduced by about 30% in 20,000 years, making it easier for vegetation to colonize, if nothing else changed over this time scale.

Identifying response times and observing their consequences requires long-term observation. This has been possible in this observatory, where both sediment and vegetation data are available over a period of 40 years. This clearly advocate for continued efforts by the scientific community and funding agencies to support long-term observation of the critical zone, such as carried out within the OZCAR network and other international erosion and critical zone observatories (Gaillardet et al, 2018, Guo and Lin, 2016).

4.4 Methodological contributions and limitations

In this study, we combined several complementary data sources to quantify vegetation dynamics and relate them to erosion processes. Historical infrared aerial photographs with high spatial resolution (0.5–1 m) but low temporal resolution (one image approximately every 10 years) were coupled with Landsat imagery, which offers higher temporal resolution (several images per year) but lower spatial resolution (30 m). This combination allowed us to reconstruct long-term vegetation trajectories while retaining information on vegetation type. Diachronic mapping from aerial photographs provided detailed land-cover transitions, revealing that pine forest, as a pioneer species, expanded and densified more rapidly than older deciduous forests and grassland. Consistent with this, both grassland and bare land preferentially transitioned to pine forest, illustrating a natural succession pathway in the absence of grazing. Linking these high-resolution land-cover transitions to Landsat NDVI trends using “pure” pixels (dominated by a single vegetation type) then allowed us to interpret remotely sensed greening patterns in terms of initial species distribution, ecological succession, and vegetation growth rather than NDVI changes alone. High-resolution, diachronic vegetation mapping thus appears to add substantial value when interpreting large-scale greening patterns from satellite data, as also highlighted by Bayle et al. (2024). A further contribution of this work is the derivation of empirical colonization and extinction probabilities from repeated high-resolution classifications. By relating these probabilities to topographic variables (slope, drainage area, elevation, aspect), erosion rates derived from LiDAR, and vegetation neighbourhood, we translate land-cover change into process-oriented metrics that directly inform mechanisms such as dispersal limitation and erosion thresholds. Finally, by combining LiDAR-based erosion estimates with long-term vegetation transitions within a well-instrumented observatory, this study illustrates how remote sensing and field-based measurements can be jointly exploited to investigate coupled vegetation–erosion dynamics in badlands.

Yet, our analysis of land-cover evolution based on infrared aerial photographs is limited by the temporal resolution: only five images are available, and one of them was excluded due to shading. This prevents us from tracking colonization and extinction

https://doi.org/10.5194/egusphere-2026-834
Preprint. Discussion started: 31 March 2026

at fine temporal scales and instead provides an integrated estimate over relatively long interval. We treated colonization and extinction as if only one change occurred between successive images, but we cannot exclude the possibility that several cycles of colonization and extinction took place within these intervals, particularly during the longer 1994–2015 period. Although the vegetation-type classification performs well overall, misclassification remains possible, especially between grassland and pine forest, which have slightly overlapped infrared signatures. Erosion estimates derived from LiDAR point cloud comparison also suffer from uncertainties. While the vertical uncertainty of individual LiDAR returns is on the order of a few centimeters, point density is a key parameter for accurately interpolating a raster surface. The main limitation here is the resolution and ground-point density of the 2021-point cloud (10 points m^{-2}), particularly in vegetated areas where fewer ground echoes are available. For this reason, our analyses are restricted to raster cells where erosion data are available, representing 88% of the denuded area and 46% of the vegetated area of the catchment. New, higher-density LiDAR acquisitions would be needed to better constrain erosion patterns, especially under vegetation. Defining the elevation of the bare surface is relatively straightforward, but doing so under vegetation is more challenging because litter and low vegetation can partially mask the ground. Classification algorithms for LiDAR point clouds typically identify the ground by selecting the lowest points, but these may correspond to litter rather than the true soil surface. Ground elevation under vegetation may therefore be overestimated, leading to larger uncertainties in erosion estimates, particularly in sectors where vegetation cover has changed over the study period.

Furthermore, our colonization and extinction probabilities are estimated at the pixel scale using a large number of spatially correlated pixels (~340 000 in total). As a consequence, formal statistical tests are influenced by both spatial dependence and very large sample sizes, and we therefore interpret results primarily in terms of effect sizes and patterns rather than strict hypothesis testing. Climate–NDVI relationships are based on “pure” Landsat pixels and thus mainly reflect the response of relatively homogeneous, stable stands, rather than the highly dynamic edges where transitions are most frequent. Finally, erosion rates are derived from LiDAR data over a relatively short period compared to the full duration of vegetation change; our interpretation assumes that the spatial pattern of erosion during this period is representative of typical conditions. Despite these limitations and uncertainties, the analysis reveals robust and coherent trends when averaging over large numbers of pixels (with at least 1 000 pixels in each vegetation or topographic class), suggesting that many of the local uncertainties are averaged out and that the main patterns we describe are reliable.

5 Conclusions

We found that vegetation has increased, both in its extent, and in total biomass, over the last 40 years, in the badlands of Draix, SE France. Spatially, vegetation dynamics appear to be controlled by geomorphic and ecological processes: First, a slope stability angle of 90% (42°) controls the transition between slowly eroding, even depositing environments, favoring colonisation, and intensely eroding slopes that favor extinction and prevent colonization. Secondly, grain-dispersion limits colonisation to short distances from existing vegetation. Moreover, greening trends are found to depend on vegetation type

https://doi.org/10.5194/egusphere-2026-834
Preprint. Discussion started: 31 March 2026

and ecological succession. This increase is correlated to an increase in temperature and precipitation, although it can not be attributed with certainty to climate change.

This study underlines the strong interactions between erosion and vegetation dynamics in this badland system. On the short-term, it demonstrates that topography and erosion are able to control vegetation dynamics patterns. On the longer term, it suggests that vegetation dynamics coupled with erosion in a tectonically active setting may produce an intrinsically instable system. Accounting for these interactions and their response time is therefore critical when modeling the co-evolution of erosion and vegetation in these badlands, and for predicting the response of badlands to climate change

Data availability

IGN aerial IR images for 1982, 1994, 2015 and 2021 are available at https://geoservices.ign.fr/bdortho

2025 LiDAR point cloud is available at https://doi.org/10.57745/DAEB1Z

2021 LiDAR point cloud is available at https://geoservices.ign.fr/lidarhd

Rainfall, temperature and sediment flux data for Laval catchment are available at https://doi.org/10.17180/obs.draix

Vegetation maps, erosion map and greening map will be available with DOI after preprint posting

Author contribution

CLB and PC designed the study

AB acquired and corrected satellite data and computed greening maps

HS produced temperature data

SK produced rainfall and sediment export data

TDA and LB performed the orthorectification with Metashape

TDA performed the vegetation classification and greening analysis with help from PC, AB and CLB

JP analyzed the LiDAR data and produced the erosion map with help from CLB

CLB wrote the paper with inputs from all other authors

Competing interests

The authors declare that they have no conflict of interest.

Acknowledgements

The research was performed in Draix-Bleone observatory, which is a national observation service (SNO) supported by CNRS-INSU, INRAE and OSUG. It is part of OZCAR-RI French research infrastructure.

AI tools were used to rephrase and improve the wording of a few sentences, representing less than 2% of the manuscript.

https://doi.org/10.5194/egusphere-2026-834
Preprint. Discussion started: 31 March 2026

Financial support

This research was funded by ANR CLIMBAD (ANR-22-CE01-0008)

References

Amundson, R., Heimsath, A., Owen, J., Yoo, K., and Dietrich, W. E.: Hillslope soils and vegetation, Geomorphology, 234, 122–132, doi:10.1016/j.geomorph.2014.12.031, 2015.

Ariagno, C., Le Bouteiller, C., van der Beek, P., and Klotz, S.: Sediment export in marly badland catchments modulated by frost-cracking intensity, Draix–Bléone Critical Zone Observatory, SE France: Earth Surf. Dynam., 10, 81–96, doi:10.5194/esurf-10-81-2022, 2022.

Ariagno, C., Pasquet, S., Le Bouteiller, C., van der Beek, P., and Klotz, S.: Seasonal dynamics of marly badlands illustrated by field records of hillslope regolith properties, Draix–Bléone Critical Zone Observatory, South-East France. Earth Surface Processes and Landforms, 48(8), 1526-1539, doi:10.1002/esp.5564, 2023

Badano, E. I., Cavieres, L. A., Molina-Montenegro, M. A., and Quiroz, C. L.: Slope aspect influences plant association patterns in the Mediterranean matorral of central Chile. Journal of Arid Environments, 62(1), 93-108, doi:10.1016/j.jaridenv.2004.10.012, 2005.

Badoux, A., Andres, N., and Turowski, J. M.: Damage costs due to bedload transport processes in Switzerland. Natural Hazards and Earth System Sciences, 14(2), 279–294, doi:10.5194/nhess-14-279-2014, 2014.

Bayle, A., Gascoin, S., Berner, L. T., and Choler, P.: Landsat-based greening trends in alpine ecosystems are inflated by multidecadal increases in summer observations. Ecography, 2024(12), e07394, doi:10.1111/ecog.07394, 2024.

Bechet, J., Duc, J., Loye, A., Jaboyedoff, M., Mathys, N., Malet, J.-P., Klotz, S., Le Bouteiller, C., Rudaz, B., and Travelletti, J. Detection of seasonal cycles of erosion processes in a black marl gully from a time series of high-resolution digital elevation models (DEMs). Earth Surface Dynamics, 4(4), 781-798, doi:10.5194/esurf-4-781-2016, 2016.

Besl, P. J., and McKay, N. D.: A method for registration of 3-D shapes. IEEE Transactions on Pattern Analysis and Machine Intelligence, 14(2), 239-256, doi:10.1109/34.121791, 1992.

Bilotta, G.S. and Brazier, R.E. Understanding the Influence of Suspended Solids on Water Quality and Aquatic Biota. Water Research, 42, 2849-2861, doi:10.1016/j.watres.2008.03.018, 2008.

Bochet, E., García-Fayos, P., and Poesen, J.: Topographic thresholds for plant colonization on semi-arid eroded slopes. Earth Surface Processes and Landforms, 34(13), 1758–1771., doi:10.1002/esp.1860, 2009.

Bochet, E., Poesen, J. and Rubio, J.L.: Runoff and soil loss under individual plants of a semi-arid Mediterranean shrubland: influence of plant morphology and rainfall intensity. Earth Surf. Process. Landforms, 31: 536-549, doi:10.1002/esp.1351, 2006.

https://doi.org/10.5194/egusphere-2026-834
Preprint. Discussion started: 31 March 2026

Boukhari, Y., Lucas, A., Le Bouteiller, C., Klotz, S., Chabaud, G., and Jacquemoud, S.: Spatial assessment of sediment production in a badland catchment using repeat LiDAR surveys, Draix, Alpes de Haute-Provence, France, Earth Surf. Dynam., 13, 1205–1228, https://doi.org/10.5194/esurf-13-1205-2025, 2025

Burylo, M., Rey, F., Roumet, C., Buisson, E., and Dutoit, T.: Linking plant morphological traits to uprooting resistance in eroded marly lands (Southern Alps, France). Plant and Soil, 324(1), 31–42, doi:10.1007/s11104-009-9920-5, 2009.

Canton, Y., Domingo, F., Sole-Benet, A., and Puigdefabregas, J. : Hydrological and erosion response of a badlands system in semiarid SE Spain. Journal of Hydrology, 252(1), 65–84, doi:10.1016/S0022-1694(01)00450-4, 2001.

Carlson, B. Z., Corona, M. C., Dentant, C., Bonet, R., Thuiller, W., and Choler, P.: Observed long-term greening of alpine vegetation—A case study in the French Alps. Environmental Research Letters, 12(11), 114006, doi:10.1088/1748-9326/aa84bd, 2017.

Carriere, A., Le Bouteiller, C., Tucker, G. E., Klotz, S., and Naaim, M.: Impact of vegetation on erosion: Insights from the calibration and test of a landscape evolution model in alpine badland catchments. Earth Surf. Process. Landforms, 45: 1085–1099, doi:10.1002/esp.4741, 2020.

Cerda, A., and García-Fayos, P.: The influence of seed size and shape on their removal by water erosion. Catena, 48(4), 293-301, doi:10.1016/S0341-8162(02)00027-9, 2002.

Choler, P., Bayle, A., Carlson, B. Z., Randin, C., Filippa, G., and Cremonese, E.: The tempo of greening in the European Alps: Spatial variations on a common theme. Global Change Biology, 27, 5614–5628, doi:10.1111/gcb.15820, 2021.

Copard, Y., F. Eyrolle, O. Radakovitch, A. Poirel, et al. : Badlands as a hot spot of petrogenic contribution to riverine particulate organic carbon to the Gulf of Lion (NW Mediterranean Sea). Earth Surf Process Landforms, 43 (12), pp.2495-2509. https://dx.doi.org/10.1002/esp.4409, 2018.

Crouzy B, Edmaier K, Perona P.: Biomechanics of plant anchorage at early development stage. J Theor Biol. 21, 363:22-9. doi: 10.1016/j.jtbi.2014.07.034, 2014.

De Frenne P, Zellweger F, Rodríguez-Sánchez F, Scheffers BR, Hylander K, Luoto M, Vellend M, Verheyen K, Lenoir J.: Global buffering of temperatures under forest canopies. Nat Ecol Evol., 3(5):744-749. doi: 10.1038/s41559-019-0842-1, 2019.

Debain, S. D., Chadœuf, J. C., Curt, T. C., Kunstler, G. K., and Lepart, J. L.: Comparing effective dispersal in expanding population of Pinus sylvestris and Pinus nigra in calcareous grassland. Canadian Journal of Forest Research. https://doi.org/10.1139/X06-265, 2007.

Descroix, L., and Mathys, N.: Processes, spatio-temporal factors and measurements of current erosion in the French Southern Alps : A review. Earth Surface Processes and Landforms, 28(9), 993-1011. https://doi.org/10.1002/esp.514, 2003.

Dietrich, W., and Perron, J.: The search for a topographic signature of life. Nature 439, 411–418, https://doi.org/10.1038/nature04452, 2006.

Eichel, J., Corenblit, D., and Dikau, R.: Conditions for feedbacks between geomorphic and vegetation dynamics on lateral moraine slopes: A biogeomorphic feedback window. Earth Surface Processes and Landforms, 41(3), 406–419. https://doi.org/10.1002/esp.3859, 2016.

https://doi.org/10.5194/egusphere-2026-834
Preprint. Discussion started: 31 March 2026

Erktan, A., Cécillon, L., Graf, F., Roumet, C., Legout, C., and Rey, F.: Increase in soil aggregate stability along a Mediterranean successional gradient in severely eroded gully bed ecosystems: combined effects of soil, root traits and plant community characteristics. Plant and Soil, 398(1/2), 121–137. http://www.jstor.org/stable/43872734, 2016.

Esteves, M., Descroix, L., Mathys, N., and Marc Lapetite, J.: Soil hydraulic properties in a marly gully catchment (Draix, France). Catena, 63(2), 282-298. https://doi.org/10.1016/j.catena.2005.06.006, 2005.

Famiglietti, J. S., Rudnicki, J. W., and Rodell, M.: Variability in surface moisture content along a hillslope transect: Rattlesnake Hill, Texas. Journal of Hydrology, 210(1-4), 259-281. https://doi.org/10.1016/S0022-1694(98)00187-5, 1998.

Gaillardet, J., Braud, I., Hankard, F., et al. : OZCAR : The French Network of Critical Zone Observatories. Vadose Zone Journal, 17: 1-24 180067. https://doi.org/10.2136/vzj2018.04.0067, 2018.

Gallardo-Cruz, J. A., Pérez-García, E. A., and Meave, J. A.: β-Diversity and vegetation structure as influenced by slope aspect and altitude in a seasonally dry tropical landscape. Landscape Ecology, 24(4), 473-482, doi:10.1007/s10980-009-9332-1, 2009.

Gallart, F., Marignani, M., Pérez-Gallego, N., Santi, E., and Maccherini, S. : Thirty years of studies on badlands, from physical to vegetational approaches. A succinct review. CATENA, 106, 4-11. https://doi.org/10.1016/j.catena.2012.02.008, 2013.

Gamba, E., Shindo, L., Isoardi, D., and Talon, B.: Multidisciplinary approach to investigate human-forest relationships in southern French Alps : How to estimate the impact of populations on the local mountain wood stock? Quaternary International, 700-701, 80-96, doi:10.1016/j.quaint.2023.07.011, 2024.

Ghahramani, A., Ishikawa, Y., and Gomi, T.: Slope length effect on sediment and organic litter transport on a steep forested hillslope : Upscaling from plot to hillslope scale. Hydrological Research Letters, 5, 16-20, https://doi.org/10.3178/hrl.5.16, 2011.

Grizonnet, M., Michel, J., Poughon, V., Inglada, J., Savinaud, M., and Cresson, R.: Orfeo ToolBox : Open source processing of remote sensing images. Open Geospatial Data, Software and Standards, 2(1), 15. https://doi.org/10.1186/s40965-017-0031-6, 2017.

Guerrero-Campo, J., Alberto, F., Hodgson, J., García-Ruiz, J. M., and Montserrat-Martí, G.: Plant community patterns in a gypsum area of NE Spain. I. Interactions with topographic factors and soil erosion. Journal of Arid Environments 41(4) pp 401-410, https://doi.org/10.1006/jare.1999.0492, 1999.

Guo, L. and Lin, H. : Critical Zone Research and Observatories: Current Status and Future Perspectives. Vadose Zone Journal 15 (9). doi: https://doi.org/10.2136/vzj2016.06.0050, 2016.

Gyssels, G., Poesen, J., Bochet, E., and Li, Y.: Impact of plant roots on the resistance of soils to erosion by water: A review. Progress in Physical Geography, 29(2), 189–217. https://doi.org/10.1191/0309133305pp443ra, 2005.

Haesen, S., Lembrechts, J. J., De Frenne, P., Lenoir, J., Aalto, J., Ashcroft, M. B., Kopecky, M., Luoto, M., Maclean, I., Nijs, I., Niittynen, P., van den Hoogen, J., Arriga, N., Bruna, J., Buchmann, N., Ciliak, M., Collalti, A., De Lombaerde, E., Descombes, P., … Van Meerbeek, K.: ForestTemp – Sub-canopy microclimate temperatures of European forests. Global Change Biology, 27, 6307–6319, 2021.

https://doi.org/10.5194/egusphere-2026-834
Preprint. Discussion started: 31 March 2026

Haralick, R. M.: Statistical and structural approaches to texture. Proceedings of the IEEE, 67(5), 786-804, doi:10.1109/PROC.1979.11328, 1979.

Herrero, A., Vila, J., Eljarrat, E., Ginebreda, A., Sabater, S., Batalla, R. J., and Barcelo, D.: Transport of sediment borne contaminants in a Mediterranean river during a high flow event. Science of The Total Environment, 633, 1392–1402. https://doi.org/10.1016/j.scitotenv.2018.03.205, 2018.

Hilton, R.G., and West, A.J.: Mountains, erosion and the carbon cycle. Nat Rev Earth Environ 1, 284–299, https://doi.org/10.1038/s43017-020-0058-6, 2020.

IGN: Lidar HD [Database]. Institut national de l'information géographique et forestière (IGN)., https://geoservices.ign.fr/lidarhd, 2024.

IPCC: Climate Change and Land: an IPCC special report on climate change, desertification, land degradation, sustainable land management, food security, and greenhouse gas fluxes in terrestrial ecosystems [P.R. Shukla, J. Skea, E. Calvo Buendia, V. Masson-Delmotte, H.-O. Pörtner, D. C. Roberts, P. Zhai, R. Slade, S. Connors, R. van Diemen, M. Ferrat, E. Haughey, S. Luz, S. Neogi, M. Pathak, J. Petzold, J. Portugal Pereira, P. Vyas, E. Huntley, K. Kissick, M. Belkacemi, J. Malley, (eds.)], 2019.

Istanbulluoglu, E., and Bras, R. L.: Vegetation-modulated landscape evolution : Effects of vegetation on landscape processes, drainage density, and topography. Journal of Geophysical Research: Earth Surface, 110(F2). https://doi.org/10.1029/2004JF000249, 2005.

Klotz, S., Le Bouteiller, C., Mathys, N., Fontaine, F., Ravanat, X., Olivier, J.-E., Liébault, F., Jantzi, H., Coulmeau, P., Richard, D., Cambon, J.-P., and Meunier, M.: A high-frequency, long-term data set of hydrology and sediment yield: the alpine badland catchments of Draix-Bléone Observatory, Earth Syst. Sci. Data, 15, 4371–4388, https://doi.org/10.5194/essd-15-4371-2023, 2023.

Knuth, F., Shean, D., Bhushan, S., Schwat, E., Alexandrov, O., McNeil, C., Dehecq, A., Florentine, C., O'Neel, S.: Historical Structure from Motion (HSfM): Automated processing of historical aerial photographs for long-term topographic change analysis, Remote Sensing of Environment, Volume 285,113379, https://doi.org/10.1016/j.rse.2022.113379, 2023.

Lague, D., Brodu, N., and Leroux, J.: Accurate 3D comparison of complex topography with terrestrial laser scanner: Application to the Rangitikei canyon (N-Z). ISPRS Journal of Photogrammetry and Remote Sensing, 82, 10-26. Doi:10.1016/j.isprsjprs.2013.04.009, 2013

Le Bouteiller, C., Legout, C. and Klotz, S.: Draix-Bleone Observatory spatial data. Doi:10.57745/RUQLJL, 2023 [dataset]

Lee, J.-T., Lin, Y.-S., Shi, C.-Y., and Lee, M.-J. : Morphological traits and root anchorage ability of native pioneer tree species for reforestation of mudstone badlands. Journal of Forest Research, 27(4), 265-273. https://doi.org/10.1080/13416979.2021.2021637, 2022.

Li, Z. and Fang, H.: Impacts of climate change on water erosion: A review. Earth-Science Reviews, 163, 94-117. https://doi.org/10.1016/j.earscirev.2016.10.004, 2016.

https://doi.org/10.5194/egusphere-2026-834
Preprint. Discussion started: 31 March 2026

Liu, L., Wang, Y., Wang, Z., Li, D., Zhang, Y., Qin, D., and Li, S.: Elevation-dependent decline in vegetation greening rate driven by increasing dryness based on three satellite NDVI datasets on the Tibetan Plateau. Ecological Indicators, 107. https://doi.org/10.1016/j.ecolind.2019.105569, 2019.

Löbmann, M. T., Geitner, C., Wellstein, C., and Zerbe, S.: The influence of herbaceous vegetation on slope stability – A review. Earth-Science Reviews, 209, 103328. https://doi.org/10.1016/j.earscirev.2020.103328, 2020.

Lucht, W., Prentice, I. C., Myneni, R. B., Sitch, S., Friedlingstein, P., Cramer, W., Bousquet, P., Buermann, W., and Smith, B.: Climatic Control of the High-Latitude Vegetation Greening Trend and Pinatubo Effect. Science. https://doi.org/10.1126/science.1071828, 2002.

Mallet, F., Marc, V., Douvinet, J., Rossello, P., Joly, D., and Ruy, S.: Assessing Soil Water Content Variation in a Small Mountainous Catchment over Different Time Scales and Land Covers Using Geographical Variables. Journal of Hydrology 591, 125593, doi:10.1016/j.jhydrol.2020.125593, 2020.

Marston, R. A.: Geomorphology and vegetation on hillslopes: Interactions, dependencies, and feedback loops. Geomorphology, 116(3–4), 206–217. https://doi.org/10.1016/j.geomorph.2009.09.028, 2010.

Mas, E., Cochard, H., Deluigi, J., Didion-Gency, M., Martin-StPaul, N., Morcillo, L., Valladares, F., Vilagrosa, A. and Grossiord, C.: Interactions between beech and oak seedlings can modify the effects of hotter droughts and the onset of hydraulic failure, New Phytol, 241: 1021-1034. https://doi.org/10.1111/nph.19358, 2024.

Mathys, N., Klotz, S., Esteves, M., Descroix, L., and Lapetite, J. M. : Runoff and erosion in the Black Marls of the French Alps : Observations and measurements at the plot scale. Catena, 63(2), 261-281. https://doi.org/10.1016/j.catena.2005.06.010, 2005

Nadal-Romero, E, Rodriguez-Caballero, E, Chamizo, S, Juez, C, Canton, Y, Garcia-Ruiz, J.M.: Mediterranean badlands: Their driving processes and climate change futures, Earth Surf. Process. Landforms 1 – 15. https://doi.org/10.1002/esp.5088, 2021.

Nadal-Romero, E., Martinez-Murillo, J. and Kuhn, N. : Badland Dynamics in the Context of Global Change, Elsevier, 2018b.

Nadal-Romero, E., Pena-Angulo, D., and Regues, D.: Rainfall, run-off, and sediment transport dynamics in a humid mountain badland area: Long-term results from a small catchment. https://doi.org/10.1002/hyp.11495, 2018a.

Nadal-Romero, E., Petrlic, K., Verachtert, E., Bochet, E., and Poesen, J.: Effects of slope angle and aspect on plant cover and species richness in a humid Mediterranean badland. Earth Surface Processes and Landforms, 39(13), 1705–1716. https://doi.org/10.1002/esp.3549, 2014.

Nearing, M., Pruski, F., and O'Neal, M.: Expected climate change impacts on soil erosion rates: A review, J. Soil Wat. Conserv., 59, 43–50, 2004.

Nemani, R. R., Keeling, C. D., Hashimoto, H., Jolly, W. M., Piper, S. C., Tucker, C. J., Myneni, R. B., and Running, S. W.: Climate-Driven Increases in Global Terrestrial Net Primary Production from 1982 to 1999. Science, 300(5625), 1560-1563. https://doi.org/10.1126/science.1082750, 2003.

Ohsawa, T., Tsuda, Y., Saito, Y. et al. : Steep slopes promote downhill dispersal of Quercus crispula seeds and weaken the fine-scale genetic structure of seedling populations. Ann. For. Sci. 64, 405–412, https://doi.org/10.1051/forest:2007017, 2007.

https://doi.org/10.5194/egusphere-2026-834
Preprint. Discussion started: 31 March 2026

Pelletier, J. D., Barron-Gafford, G. A., Gutiérrez-Jurado, H., Hinckley, E.-L. S., Istanbulluoglu, E., McGuire, L. A., Niu, G.-Y., Poulos, M. J., Rasmussen, C., Richardson, P., Swetnam, T. L., and Tucker, G. E.: Which way do you lean? Using slope aspect variations to understand Critical Zone processes and feedbacks. Earth Surface Processes and Landforms, 43(5), 1133-1154, doi:10.1002/esp.4306, 2018.

Pepin, N., Bradley, R. S., Diaz, H. F., Baraer, M., Caceres, E. B., Forsythe, N., Fowler, H., Greenwood, G., Hashmi, M. Z., Liu, X. D., Miller, J. R., Ning, L., Ohmura, A., Palazzi, E., Rangwala, I., Schöner, W., Severskiy, I., Shahgedanova, M., Wang, M. B., … Yang, D. Q.: Elevation-dependent warming in mountain regions of the world. Nature Climate Change, 5(5), 424–430. Scopus. https://doi.org/10.1038/nclimate2563, 2015.

Reuber, V. M., Westbury, M. V., Rey-Iglesia, A., Asefa, A., Farwig, N., Miehe, G., Opgenoorth, L., Sumbera, R., Wraase, L., Wube, T., Lorenzen, E. D., and Schabo, D. G.: Topographic barriers drive the pronounced genetic subdivision of a range-limited fossorial rodent. Molecular Ecology, 33, e17271, 2024.

Richardson, P. W., Perron, J. T., and Schurr, N. D.: Influences of climate and life on hillslope sediment transport, Geology, 47(5), 423–426. https://doi.org/10.1130/G45305.1, 2019.

Richardson, P. W., Perron, J. T., Miller, S. R., and Kirchner, J. W.: Unraveling the Mysteries of Asymmetric Topography at Gabilan Mesa, California. Journal of Geophysical Research: Earth Surface, 125(7), https://doi.org/10.1029/2019JF005378, 2020.

Rovera, G., and Robert, Y. : Conditions climatiques hivernales et processus d'érosion périglaciaires dans les bad-lands marneux de Draix (800 m, Alpes du Sud, France). Géographie physique et Quaternaire, 59(1), 31-48. https://doi.org/10.7202/013735ar, 2005.

Rumpf, S. B., Gravey, M., Brönnimann, O., Luoto, M., Cianfrani, C., Mariethoz, G., and Guisan, A.: From white to green: Snow cover loss and increased vegetation productivity in the European Alps. Science, 376(6597), 1119–1122. https://doi.org/10.1126/science.abn6697, 2022.

Samonil, P., Jaros, J., Danek, P., Tikhomirov, D., Novotny, V., Weiblen, G., Christl, M., and Egli, M.: Soil erosion affected by trees in a tropical primary rain forest, Papua New Guinea. Geomorphology, 425, 108589. https://doi.org/10.1016/j.geomorph.2023.108589, 2023.

Sharma, H., Ehlers, T. A., Glotzbach, C., Schmid, M., and Tielborger, K.: Effect of rock uplift and Milankovitch timescale variations in precipitation and vegetation cover on catchment erosion rates, Earth Surf. Dynam., 9, 1045–1072. https://doi.org/10.5194/esurf-9-1045-2021, 2021.

Syvitski JP, Vörösmarty CJ, Kettner AJ, Green P.: Impact of humans on the flux of terrestrial sediment to the global coastal ocean. Science 308(5720):376-80. doi: 10.1126/science.1109454, 2005.

Thompson, S., and Katul, G.: Secondary seed dispersal and its role in landscape organization. Geophysical Research Letters, 36(2). Scopus. https://doi.org/10.1029/2008GL036044, 2009.

Torri, D., Santi, E., Marignani, M., Rossi, M., Borselli, L., and Maccherini, S.: The recurring cycles of biancana badlands: Erosion, vegetation and human impact. CATENA, 106, 22-30. https://doi.org/10.1016/j.catena.2012.07.001, 2013.

https://doi.org/10.5194/egusphere-2026-834
Preprint. Discussion started: 31 March 2026

Vallauri, D. R., Aronson, J., and Barbero, M.: An analysis of forest restoration 120 years after reforestation on badlands in the Southwestern Alps. Restoration Ecology, 10(1), 16–26. https://doi.org/10.1046/j.1526-100X.2002.10102.x, 2002.

Vázquez-Tarrío, D., Ruiz-Villanueva, V., Garrote, J., Benito, G., Calle, M., Lucía, A., and Díez-Herrero, A.: Effects of sediment transport on flood hazards: Lessons learned and remaining challenges. Geomorphology, 446, 108976. https://doi.org/10.1016/j.geomorph.2023.108976, 2024.

Walde, M. G., Gessler, A., and Vitasse, Y.: Effects of reduced precipitation and advanced spring phenology on intra - and interspecific competition between beech, oak and linden saplings. Journal of Ecology, 114, e70231. https://doi.org/10.1111/1365-2745.70231, 2026.

Yetemen, O., Saco, P. M., and Istanbulluoglu, E.: Ecohydrology controls the geomorphic response to climate change. Geophys. Res. Letters, 46, 8852– 8861. https://doi.org/10.1029/2019GL083874, 2019.

Yin, G., Xie, J., Ma, D., Xie, Q., Verger, A., Descals, A., Filella, I., and Penuelas, J. : Aspect Matters: Unraveling Microclimate Impacts on Mountain Greenness and Greening. Geophysical Research Letters, 50(24), https://doi.org/10.1029/2023GL105879, 2023.

Zhu, Z., Piao, S., Myneni, R. B., Huang, M., Zeng, Z., Canadell, J. G., Ciais, P., Sitch, S., Friedlingstein, P., Arneth, A., Cao, C., Cheng, L., Kato, E., Koven, C., Li, Y., Lian, X., Liu, Y., Liu, R., Mao, J., … Zeng, N.: Greening of the Earth and its drivers. Nature Climate Change, 6(8), 791–795, doi:10.1038/nclimate3004, 2016.

Zittis, G., Bruggeman, A., and Lelieveld, J.: Revisiting future extreme precipitation trends in the Mediterranean. Weather and Climate Extremes, 34, doi:10.1016/j.wace.2021.100380, 2021.